

# **Design of Plate Heat Exchangers for use in Medium Temperature Organic Rankine Cycle**

Pratiksha Gwalwanshi  
ME20M037

Akshay Kokane  
ME20M010

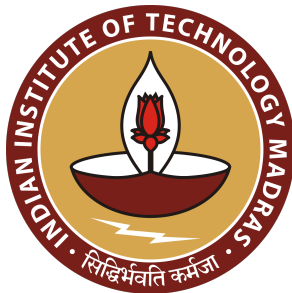
Dheerendra Mishra  
AM19S300

Guide

Dr. Satya Narayanan Seshadri  
Professor  
Department of Applied Mechanics  
IIT Madras  
satya@iitm.ac.in

January 22, 2021

INDIAN INSTITUTE OF TECHNOLOGY MADRAS



# Contents

<b>1</b>	<b>Introduction</b>	<b>i</b>
<b>2</b>	<b>System Explanation</b>	<b>i</b>
<b>3</b>	<b>Stage-1 of Validation</b>	<b>ii</b>
3.1	Initial Condition . . . . .	iii
3.2	State Point Estimation . . . . .	iv
3.3	Estimation of Areas . . . . .	iv
3.4	Condensation Heat Transfer Coefficient . . . . .	v
3.5	Evaporative or Boiling heat transfer coefficient . . . . .	vi
3.6	Exhaust Heat Transfer Coefficient . . . . .	vii
3.7	Heat Transfer Coefficient on the working fluid side in Preheater . . . . .	vii
3.8	Heat Transfer Coefficient on the working fluid side in Superheater . . . . .	vii
<b>4</b>	<b>Results</b>	<b>viii</b>
4.1	Estimated and Validated Area . . . . .	viii
4.2	Estimation and Validation of Evaporative heat transfer coefficient . . . . .	viii
4.3	Validation of Condensation heat transfer coefficient . . . . .	ix
4.4	Effects of Inlet turbine condition on evaporative heat transfer coefficient and Heat Flux . . . . .	x
<b>5</b>	<b>Stage-2 of Validation</b>	<b>xii</b>
5.1	Including Pressure Drop in Evaporator and Condenser . . . . .	xii
5.2	Applying Motinski heat transfer coefficient correlation . . . . .	xiii
5.3	Estimated Component Area . . . . .	xiv
<b>6</b>	<b>Conclusion</b>	<b>xiv</b>
<b>7</b>	<b>Annexure</b>	<b>xvi</b>

# Nomenclature

Symbol	Meaning	Symbol	Meaning
A	Heat transfer surface area( $m^2$ )	b	Height of the Corrugation(m)
Bd	Bond number	Bo	Boiling Number
$C_p$	Specific heat capacity(kJ/kgK)	Co	Convection number
$d_{eq}$	Equivalent diameter(m)	$d_h$	Hydraulic Diameter(m)
f	Friction factor	G	Mass Flux( $kg/m^2s$ )
h	Heat transfer coefficient( $kW/m^2K$ )	k	Thermal Conductivity ( $kW/mK$ )
L	Length(m)	$\dot{m}$	Mass Flow rate(kg/s)
Nu	Nusselt number	P	Pressure(Pa)
$P_{co}$	Corrugation Pitch (m)	Pr	Prandtl Number
q	Heat Flux( $kW/m^2$ )	Q	Heat Flow Rate(kW)
Re	Reynolds Number	T	Temperature(K)
t	Plate Thickness(m)	$\Delta T_{lm}$	Logarithmic Mean Temperature Difference(K)
W	Width(m)	x	Vapor Quality
$\beta$	Chevron Angle(radian)	$\rho$	Density( $kg/m^3$ )
$\mu$	Viscosity (Pa-s)	$\sigma$	Surface Tension
$\phi$	Area enlargement factor	c	Cold
con	Condenser	eq	Equivalent
exh	Exhaust	h	Hot
in	Inlet	l	Liquid Phase
out	Outlet	v/g	Vapor/Gas
w	Wall	We	Effective Width(m)

## 1 Introduction

The organic Rankine cycle is an alternate form of the Rankine cycle, most often used when the high temperatures required to produce steam are not available. The ordinary Rankine cycle uses thermal power to convert water to steam, which expands through a turbine in order to generate electricity. However, instead of using water, which has a relatively high boiling point, the organic Rankine cycle makes use of an organic fluid that has a much lower boiling point than water [1]. Toluene and Benzene are used as organic fluid in this analysis, which have boiling points as 111°C and 80°C respectively.

The objectives of this paper are-[3]

(1)-Finding out the area of heat exchangers (mainly Preheater, Evaporator, Superheater and Condenser) using LMTD method.

(2)-Finding out the variation of heat transfer coefficient (h) with respect to quality (x) using various correlations like the Shah, Han et al., Akers et al., Yan et al. and Kuo et al.

## 2 System Explanation

In this system, high temperature of the exhaust gas from the marine diesel engine has been utilized to vapourize the organic fluid (Toluene and Benzene) in order to run the organic Rankine cycle and obtain the power output from the turbine.

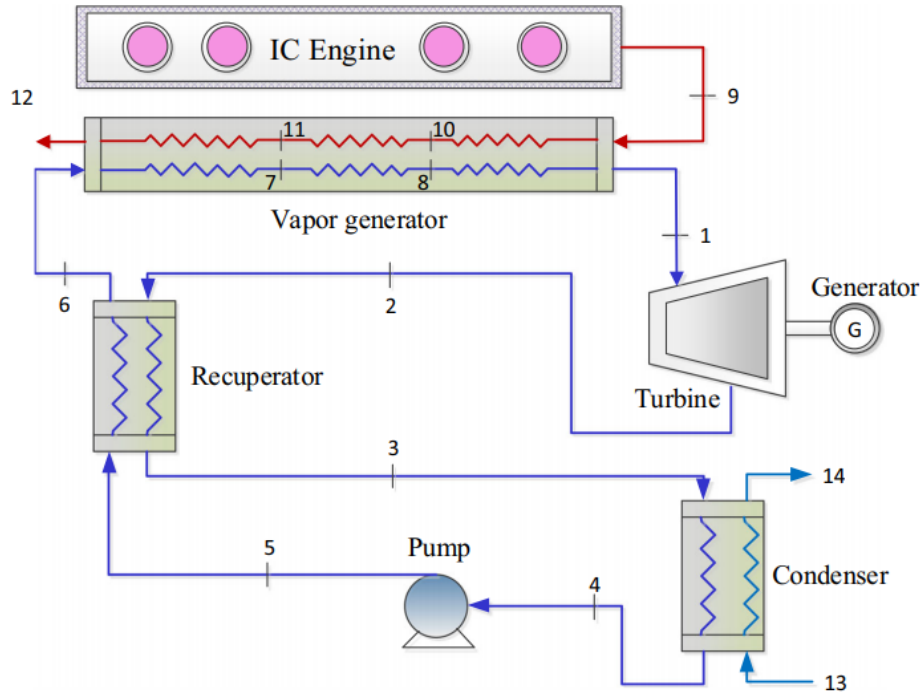


Figure 1: Organic Rankine Cycle

All the components and points are shown clearly in the above and below figure respectively. The vapour form of the organic fluid has entered the turbine at point 1 and exited at point 2. Waste heat from the turbine has been utilized to preheat the fluid exited from the pump. So the waste heat from the turbine has entered the recuperator at point 2 and exited at point 3. Heat has been transferred from the waste heat of the turbine to the liquid form of the organic fluid exited from the pump. So point 5 and point 6 represent the entry and exit points respectively, of the liquid form of the organic fluid in the recuperator.

From point 6 to point 1, it has been divided into three parts. The first part has been taken from point 6 to point 7, where the liquid form of the organic fluid has been heated. The second part has been taken from point 7 to point 8, where the latent heat of vapourization has been transferred by the waste heat from the marine diesel engine and the last part has been taken from point 8 to point 1, where vapour has been superheated. In the condenser, water has been used to extract the latent heat of condensation of the vapour form of the organic fluid and due to this; vapour has been condensed into the liquid form. This process has happened between point 3 and point 4.

### 3 Stage-1 of Validation

The main simulation program for the ORC system is written in Python, and the thermodynamic properties and the transport properties of the working fluid are obtained using CoolProp. The elemental and physical properties of the exhaust gas, here diesel [2], are taken constant at atmospheric pressure and exhaust temperature.

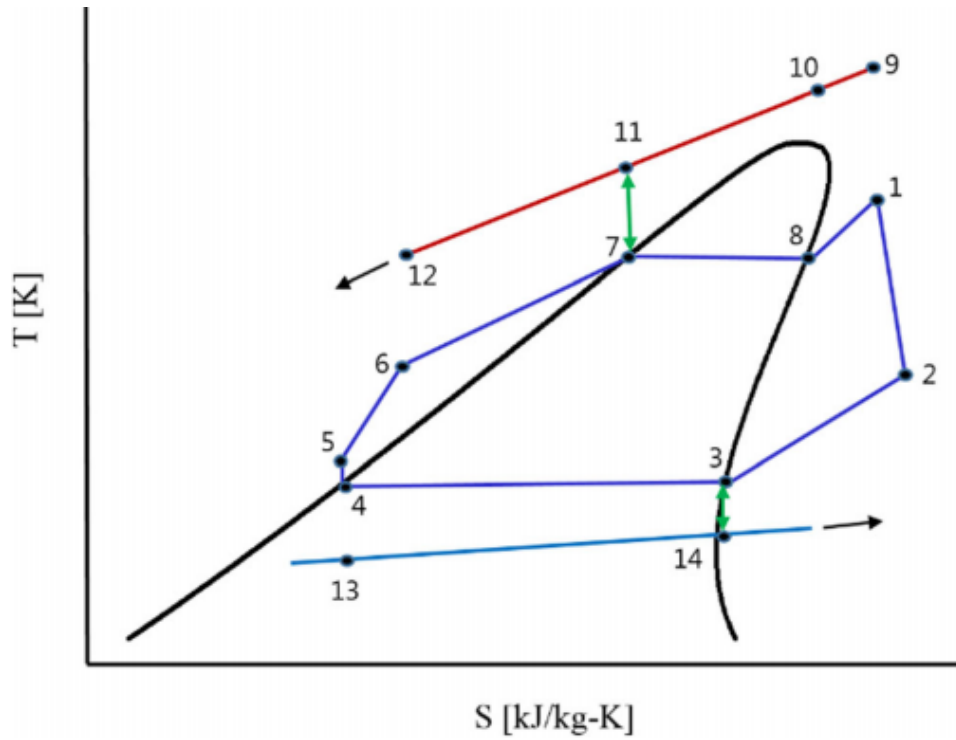


Figure 2: T-S Diagram

### 3.1 Initial Condition

The initial conditions are already given for exhaust gas and for other processes of the organic Rankine cycle. The same is shown in the table Table 1. We obtained all the state points with the use of basic heat transfer equations. Here,  $T$  represents the temperature and the subscript  $ex$  stands for the exhaust gas. The basic data can be understood from their units.

Data	Value	Data	Value
$T_1$	543 K	$T_9$	587 K
$T_7=T_8$	463 K	$m_{ex}$	105.5 kg
$P_4$	45000 Pa	$C_{ex}$	1048.2 J/kgK
$T_{13}$	298 K	$d_{ex}$	0.59508 kg/m <sup>3</sup>
$T_{11}$	$T_7+30$ K	$h_{ex}$	593967 W/m <sup>2</sup> K
$\beta$	60 degree	$v_{ex}$	.000030132 Pa-s
$b$	0.0022 m	$k_{ex}$	0.045794 W/mK
$P_{co}$	0.01325 m	$t$	0.0005 m
$W_e$	0.55 m	$k$	17 W/mK

Table 1: Initial Condition

State Points			
For Benzene		For Toluene	
Temperature	Value	Temperature	Value
$T_1$	543K	$T_1$	543K
$T_2$	438.028K	$T_2$	474.670K
$T_3$	328.988K	$T_3$	357.453K
$T_4$	328.988K	$T_4$	357.453K
$T_5$	329.314K	$T_5$	357.618K
$T_6$	417.624K	$T_6$	452.409K
$T_7$	463K	$T_7$	463K
$T_8$	463K	$T_8$	463K
$T_9$	587K	$T_9$	587K
$T_{10}$	554.907K	$T_{10}$	555.569K
$T_{11}$	493 K	$T_{11}$	493 K
$T_{12}$	470.524K	$T_{12}$	487.855K
$T_{13}$	298K	$T_{13}$	298K
$T_{14}$	318.988K	$T_{14}$	347.453K

Table 2: Estimated Temperature for Benzene and Toluene

### 3.2 State Point Estimation

We have used the initial condition, energy balance equations and CoolProp properties through Python for finding out the state points. All the state Points are shown in the above table Table 2.

### 3.3 Estimation of Areas

The areas of heat exchangers involved in this analysis are obtained through LMTD method. Formulas used for every heat exchanger are same.

$$d_h = 4 * \frac{ChannelFlowArea}{WettedParameter} = \frac{4 * b * L_w}{2 * L_w * \psi} = \frac{2 * b}{\psi}$$

$$\psi = \frac{1}{6} [1 + (1 + X^2)^{\frac{1}{2}} + 4 * (1 + \frac{X^2}{2})^{\frac{1}{2}}]$$

X is a dimensionless corrugation parameter given by,

$$X = b * \frac{\pi}{P_{co}}$$

The equivalent diameter is as follows

$$d_{eq} = 2 * b$$

The mass flux is defined by the following equation

$$G = \frac{\dot{m}}{W_e * b}$$

For overall heat transfer coefficient,

$$\frac{1}{U} = \frac{1}{h_c} + \frac{t}{k} + \frac{1}{h_h}$$

$$\Delta T_{lm} = \frac{(T_{h,in} - T_{c,out}) - (T_{h,out} - T_{c,in})}{\ln \left[ \frac{T_{h,in} - T_{c,out}}{T_{h,out} - T_{c,in}} \right]}$$

The heat transfer surface area for each component is obtained by the following equation.

$$A = \frac{Q}{U(\Delta T_{lm})}$$

So here the important parameter for calculating the heat transfer area is an overall heat transfer coefficient which depends on the convective heat transfer coefficient of hot and cold fluid. This has been obtained using the various correlations for convective heat transfer coefficient of hot and cold fluid.

### 3.4 Condensation Heat Transfer Coefficient

Five different correlations are used for estimating the heat transfer coefficient of cold fluid for the condenser. We have taken the maximum value out of these five correlations

**(1)-Yan et al.**

$$h_{cond} = 4.118 * \left( \frac{k_l}{d_h} \right) * Re_{eq}^{\frac{2}{5}} * Pr_l^{\frac{1}{3}}$$

where,

$$Re_{eq} = G_{eq} * \frac{d_h}{\mu_l}$$

where,

$$G_{eq} = G \left[ (1-x) + x * \left( \frac{\rho_l}{\rho_g} \right)^{\frac{1}{2}} \right]$$

**(2)-Akers et al.**

$$h_{cond} = 5.03 * \left( \frac{k_l}{d_h} \right) * Re_{eq}^{\frac{1}{3}} * Pr_l^{\frac{1}{3}}$$

**(3)-Shah**

$$h_{cond} = h_l \left[ (1-x)^{0.8} + \frac{3.8 * x^{0.76} * (1-x)^{0.04}}{P^{0.38}} \right]$$

**(4)-Han et al.**

$$h_{cond} = G_{e1} * \left( \frac{k_l}{d_h} \right) * Re_{eq}^{G_{e2}} * Pr_l^{\frac{1}{3}}$$

where,

$$G_{e1} = 11.22 * \left( \frac{P_{co}}{d_h} \right)^{-2.83} \left( \frac{P_{co}}{d_h} - \beta \right)^{-4.5}$$

and

$$G_{e2} = 0.35 * \left( \frac{P_{co}}{d_h} \right)^{0.23} \left( \frac{P_{co}}{d_h} - \beta \right)^{-1.48}$$

**(5)-Kuo et al.**

$$h_{cond} = 0.2092 * \left(\frac{k_l}{d_h}\right) * Re_l^{0.78} * \left(\frac{k_l}{d_h}\right)^{0.14} * Pr_l^{\frac{1}{3}} (0.25Co^{-0.45} Fr_l^{0.25} + 75Bo^{0.75})$$

where,

$$Co = \left(\frac{\rho_v}{\rho_l}\right) \left(\frac{\rho_v}{\rho_l}\right)^{0.8}$$

### 3.5 Evaporative or Boiling heat transfer coefficient

Four different correlations are used for estimating the heat transfer coefficient of cold fluid for evaporator. We have taken the maximum value out of these four correlations.

**(1)-kim et al:**

$$h_{ev} = 5.323 * \left(\frac{k_l}{d_h}\right) * Re_{eq}^{0.42} * Pr_l^{\frac{1}{3}}$$

**(2)-Han et al**

$$h_{ev} = G_{e1} * \left(\frac{k_l}{d_h}\right) * Bo_{eq}^{0.3} * Re_{eq}^{G_{e2}} * Pr_l^{0.4}$$

where,

$$G_{e1} = 2.81 * \left(\frac{P_{co}}{d_h}\right)^{-0.041} \left(\frac{P_{co}}{d_h}\right)^{-2.83} \text{ and } G_{e2} = 0.746 * \left(\frac{P_{co}}{d_h}\right)^{0.61} \left(\frac{P_{co}}{d_h}\right)^{-0.082}$$

**(3)-Donowski and Kandlikar:**

Correlation-1,

$$h_{ev} = [1.184Co^{-0.3} + 225.5Bo^{2.8}](1-x)^{0.003} * \left(\frac{k_l}{d_h}\right) * Nu_{lo}$$

Correlation-2,

$$h_{ev} = 1.055[1.056Co^{-0.4} + 1.02Bo^{0.9}](x)^{-0.12} * \left(\frac{k_l}{d_h}\right) * Nu_{lo}^{0.98}$$

where,

$$Nu_{lo} = 0.2875Re_{lo}^{0.78} * Pr_l^{\frac{1}{3}}$$

**(4)-Amalfi et al.**

For  $Bd < 4$ ,

$$h_{ev} = 982 \left(\frac{k_l}{d_h}\right) \left(\frac{k_l}{d_h}\right)^{1.101} \left(\frac{k_l}{d_h}\right)^{0.315} \left(\frac{k_l}{d_h}\right)^{-0.224} * Bo^{0.320}$$

for  $Bd > 4$ ,

$$h_{ev} = 18.495 \left(\frac{k_l}{d_h}\right) \left(\frac{k_l}{d_h}\right)^{0.248} \left(\frac{k_l}{d_h}\right)^{0.135} \left(\frac{k_l}{d_h}\right)^{0.351} * \left(\frac{k_l}{d_h}\right)^{0.223} * Bd^{0.235} * Bo^{0.198}$$

where,

$$Bd = (\rho_l - \rho_g) * g \frac{d_h^2}{\sigma}$$

and

$$Bo = \frac{q}{G * h_{fg}}$$



### 3.6 Exhaust Heat Transfer Coefficient

$$f_{exh} = (1.82 \log(Re_{exh}) - 1.64)^{-2}$$

$$h_{exh} = \frac{Nu_{exh} * K_{exh}}{d_{eq}}$$

when  $Re_{exh} < 10000$ ,

$$Nu_{exh} = \left(\frac{f_{exh}}{8}\right) * Re_{exh} * \frac{Pr_{exh}}{[12.7 \left(\frac{f_{exh}}{8}\right)^{0.5} (Pr_{exh}^{\frac{2}{3}} - 1) + 1.07]}$$

when  $10000 < Re_{exh} < 5 * 10^6$ ,

$$Nu_{exh} = \left(\frac{f_{exh}}{8}\right) * (Re_{exh} - 1000) * \frac{Pr_{exh}}{[12.7 \left(\frac{f_{exh}}{8}\right)^{0.5} (Pr_{exh}^{\frac{2}{3}} - 1) + 1.07]}$$

### 3.7 Heat Transfer Coefficient on the working fluid side in Preheater

$$Nu_l = (0.0154\beta + .1298) * Re_l^{(0.1892\beta + 0.6398)} * Pr_l^{0.35} * \left(\frac{\mu_l}{\mu_w}\right)^{0.14}$$

where,

$$Re_l = G * \frac{d_{eq}}{\mu_l}$$

$$Pr_l = \mu_l * \frac{c p_l}{k_l}$$

$$Nu_l = h_l * \frac{d_{eq}}{k_l}$$

$$h_l = Nu_l * \frac{k_l}{d_{eq}}$$

### 3.8 Heat Transfer Coefficient on the working fluid side in Superheater

$$Nu_g = 0.122 * Pr_g^{\frac{1}{3}} * \left(\frac{\mu_g}{\mu_w}\right)^{\frac{1}{6}} * (f * Re_g^2 * \sin 2\beta)^{0.374}$$

where,

$$\frac{1}{f^{0.5}} = \frac{\cos \beta}{(0.18 \tan \beta + 0.36 \sin \beta + \frac{f_0}{\cos \beta})^{0.5}} + \frac{(1 - \cos \beta)}{(3.8 f_1)^{0.5}}$$

when,  $Re_g < 2000$ ,

$$f_0 = \frac{64}{Re_g}, f_1 = \frac{579}{Re_g} + 3.85$$

when,  $Re_g > 2000$ ,

$$f_0 = (1.81 \log(Re_g) - 1.5)^{-2}, f_1 = \frac{39}{Re_g^{0.298}}$$

$$Re_g = G * \frac{d_{eq}}{\mu_g}$$

$$Pr_g = \mu_g * \frac{cp_g}{k_g}$$

$$Nu_g = h_g * \frac{d_{eq}}{k_g}$$

$$h_g = Nu_g * \frac{k_g}{d_{eq}}$$

## 4 Results

### 4.1 Estimated and Validated Area

The component heat transfer areas obtained in the paper are shown in the figure below Figure 3. The heat transfer area is roughly same for the Preheater and Superheater which is about  $67m^2$  with both Benzene and Toluene as working fluids. With Benzene, the Evaporator area is nearly  $132m^2$  and with Toluene it is around  $133m^2$ . The Condenser heat transfer area is almost  $246m^2$  for Benzene whereas  $244m^2$  for Toluene.

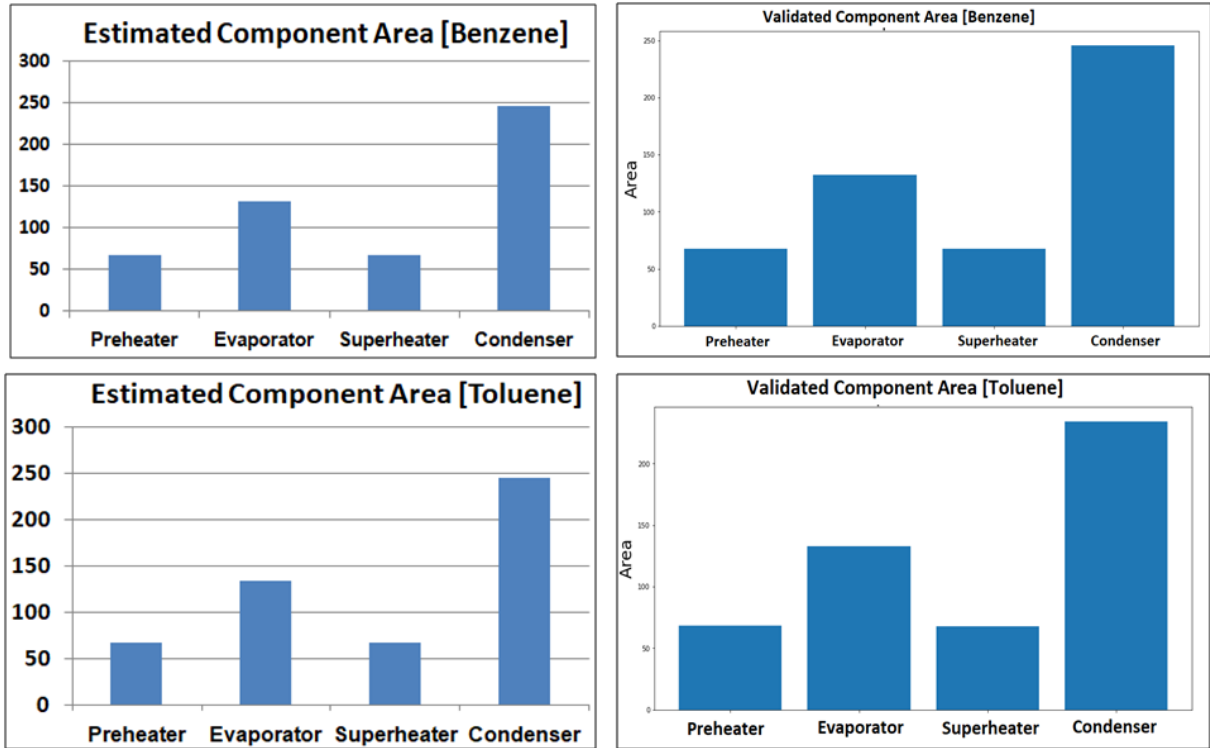


Figure 3: Estimated and Validated Area of all heat exchangers for Benzene and Toluene

### 4.2 Estimation and Validation of Evaporative heat transfer coefficient

The evaporation heat transfer coefficient is found out using several correlations as shown in the figure below Figure 4. The same is validated as shown in also Figure 4. Out of all these correlations, the Han et al. predicts the most nearby evaporation heat transfer coefficient values for

Toluene and Benzene as working fluid. Kim et al. shows almost the same results for Benzene and Toluene at low vapor quality. However, with the increase in vapor quality, the heat transfer coefficient value rises significantly for Toluene. In case of the correlation of Donowski and Kandlikar, there's hardly any variation with the vapor quality but the values are higher for Benzene than Toluene.

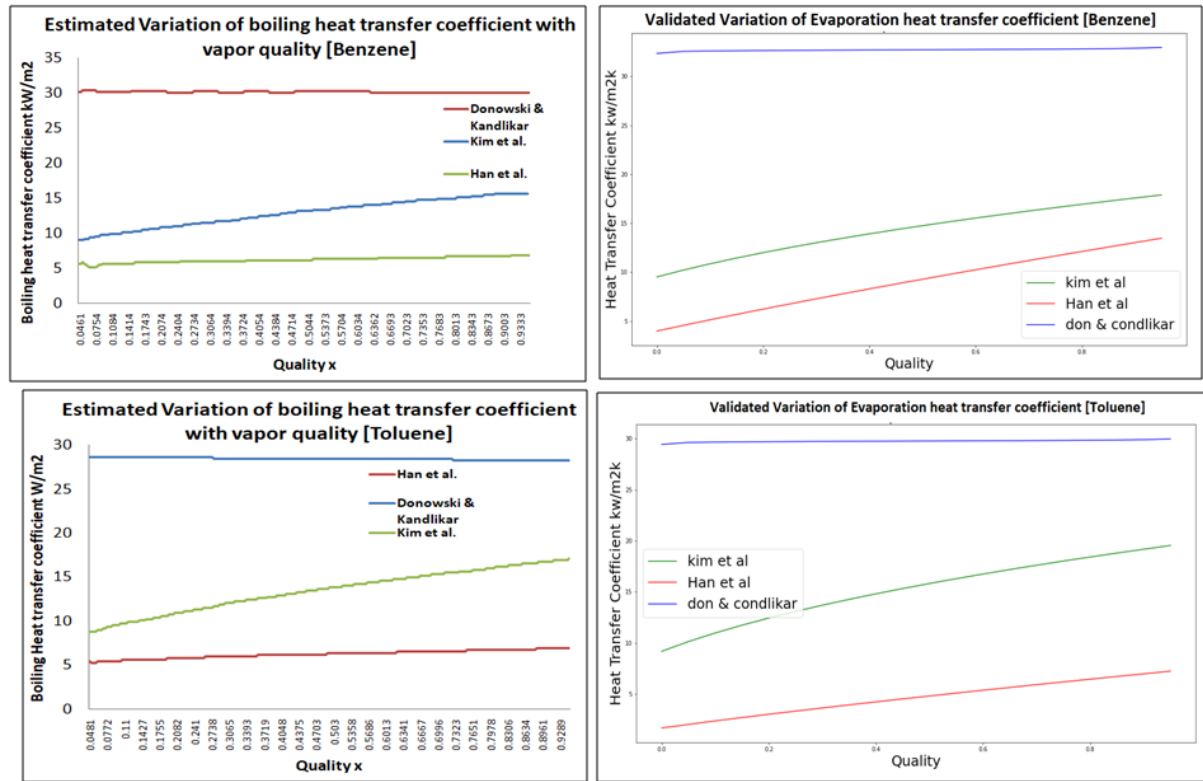


Figure 4: Estimated and Validated Evaporative heat transfer correlations for Benzene and Toluene

### 4.3 Validation of Condensation heat transfer coefficient

The condensation heat transfer coefficient is found out using several correlations as shown in the figure below Figure 5. The same is validated as shown in also Figure 5. The Shah and Akers et al. correlation gives almost the same values of condensation heat transfer coefficient with both Toluene and Benzene as the working fluid. On the other hand, the correlation of Yan et al., Kuo et al. and Han et al. predicts slightly higher values with Toluene than Benzene. The lowest heat transfer coefficient values are achieved by Shah and Han et al. correlations. The Shah correlation does not consider the effect of geometrical parameters as it is developed from extensive experimental data and is the most widely used correlation in the plate heat exchanger.

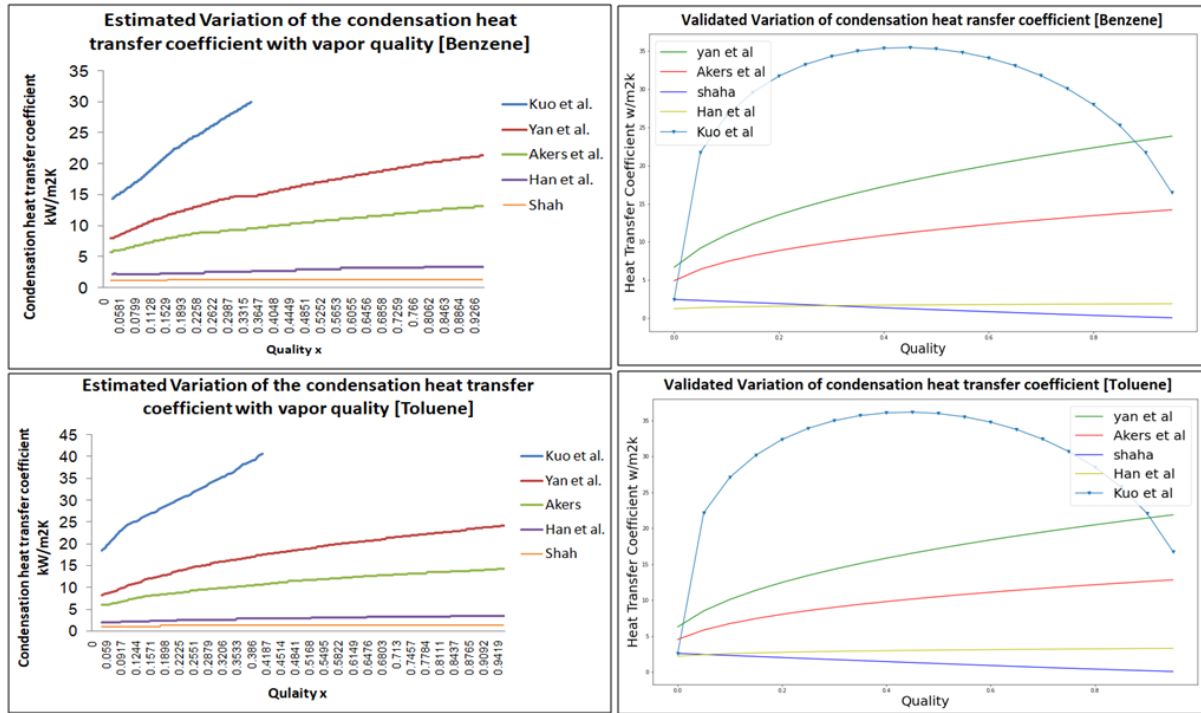


Figure 5: Variation of Condensation heat transfer coefficient with vapour quality for Benzene and Toluene

#### 4.4 Effects of Inlet turbine condition on evaporative heat transfer coefficient and Heat Flux

We noticed the effect of Turbine inlet temperature  $T_1$  on the evaporation heat transfer coefficient as shown in the figure below Figure 6. We also validated the same in Figure 6. It can be observed clearly that the evaporation heat transfer coefficient increases with a decrease in turbine inlet temperature. As the Turbine inlet temperature decreases, the exhaust temperature at the evaporator entry increases, which leads to a higher amount of heat supply to the evaporator. This is shown in the figure below Figure 7 and also the validated variation is shown in Figure 7.

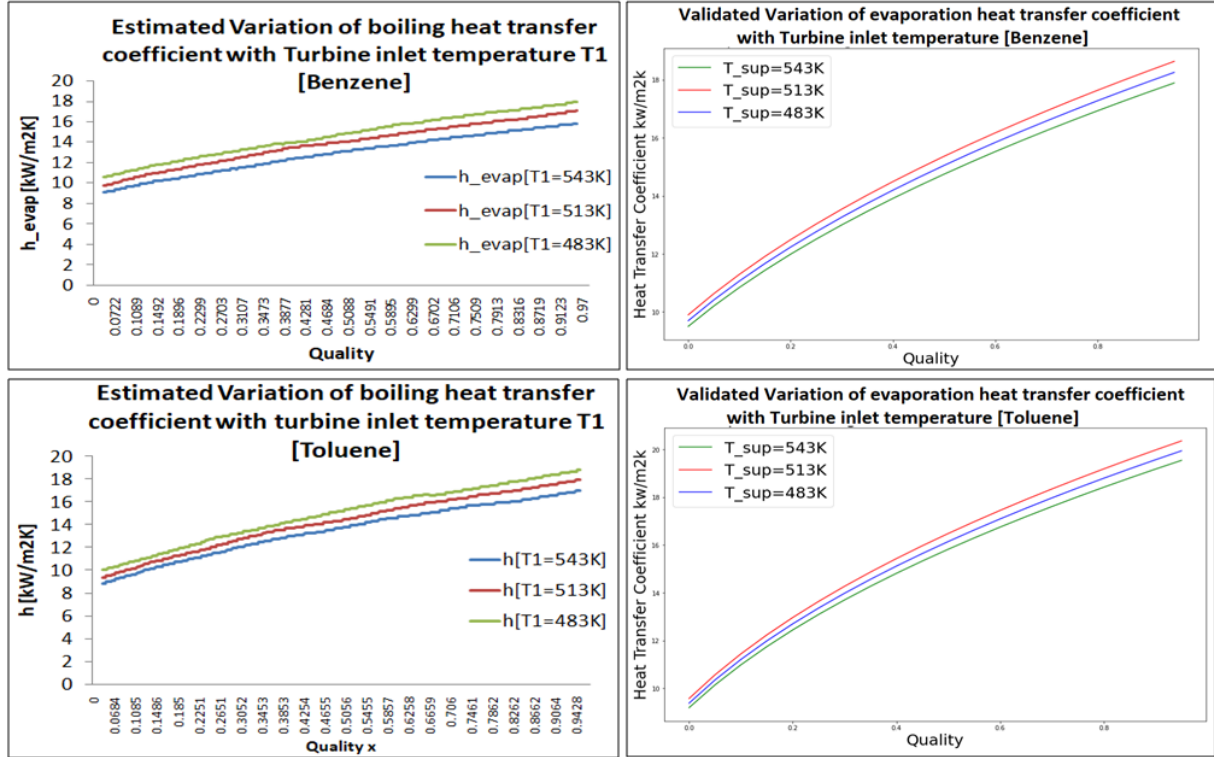


Figure 6: Variation of Evaporative/Boiling heat transfer coefficient with vapour quality, given Inlet temperature of turbine.

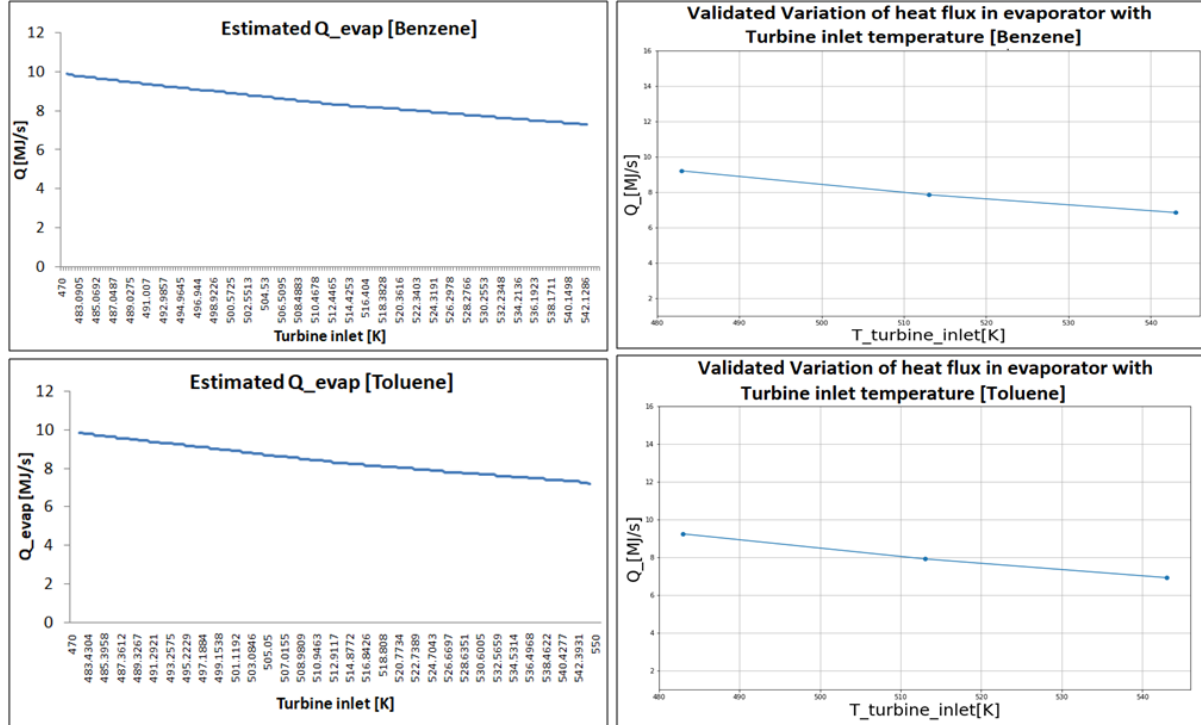


Figure 7: Variation of Heat Flux with respect to turbine inlet temperature for Toluene and Benzene

## 5 Stage-2 of Validation

### 5.1 Including Pressure Drop in Evaporator and Condenser

In the next stage of the validation we included the two phase pressure drops in evaporator and condenser. We assumed that all the other state points and properties remain same as in the case without pressure drop. This led to a lower temperature at the evaporator exit  $T_8$  and a higher temperature at the condenser entry  $T_3$ . We observed that the ratio of viscosity in the liquid form to the vapor form of the working fluid is far less than 1000 which makes the Friedel correlation to qualify for the use of frictional pressure drop for both Benzene and Toluene.

We have also included the pressure drop due to the momentum which reflects the change in the kinetic energy of the flow.

Assuming that the tubes are horizontal, we've neglected the static pressure drop.

$$\Delta P_{total} = \Delta P_{static} + \Delta P_{momentum} + \Delta P_{frictional}$$

$$\Delta P_{momentum} = \dot{m}_{total}^2 \left[ \left( \frac{(1-x)^2}{\rho_L * (1-\epsilon)} + \frac{x^2}{\rho_G * \epsilon} \right)_{out} - \left( \frac{(1-x)^2}{\rho_L * (1-\epsilon)} + \frac{x^2}{\rho_G * \epsilon} \right)_{in} \right]$$

where  $\dot{m}_{total}$  is the total mass velocity of liquid plus vapor and x is the vapor quality.

In the present study, the void fraction ( $\epsilon$ ) is obtained from steiner version of the drift flux model of Rouhani and Axelsson for horizontal tubes:

$$\epsilon = \frac{x}{\rho_G} \left[ (1 + 0.12(1-x)) \left( \frac{x}{\rho_G} + \frac{(1-x)}{\rho_L} \right) + \frac{1.18 * (1-x) [g * \sigma (\rho_L - \rho_G)]^{0.25}}{\dot{m}_{total}^2 * \rho_L^{0.5}} \right]^{-1}$$

**Frictional two phase pressure drop Friedel correlation-** This method utilizes a two phase multiplier as:-

$$\Delta P_{frictional} = \Delta P_L * \Phi_{LO}^2$$

where  $\Delta P_L$  is calculated for the liquid phase as-

$$\Delta P_L = 4f_l \left( \frac{L}{d_i} \right) \dot{m}_{total}^2 (1-x)^2 \left( \frac{1}{2\rho_L} \right)$$

The liquid friction factor and liquid Reynolds number are obtained from

$$f = \frac{0.079}{Re_e^{0.25}}$$

$$Re_e = \frac{G * d_i}{\mu}$$

Using the liquid dynamic viscosity  $\mu_L$ . His two-phase multiplier is correlated as :

$$\Phi_{LO}^2 = E + \frac{3.24FH}{Fr_h^{0.045} We_L^{0.035}}$$

where  $Fr_h$ , E, F and H are as follows:

$$Fr_h = \frac{\dot{m}_{total}^2}{gd_i \rho_h^2}$$

$$E = (1-x)^2 + x^2 \frac{\rho_L f_G}{\rho_G f_L}$$

$$F = x^{0.78} (1-x)^{0.224}$$

$$H = \left(\frac{\rho_L}{\rho_G}\right)^{0.91} \left(\frac{\mu_G}{\mu_L}\right)^{0.19} \left(1 - \frac{\mu_G}{\mu_L}\right)^{0.7}$$

The liquid Weber  $We_L$  is defined as :

$$We_L = \frac{\dot{m}_{total}^2 d_i}{\sigma \rho_h}$$

and the homogeneous density  $\rho_h$  is used:

$$\rho_h = \left(\frac{x}{\rho_G} + \frac{1-x}{\rho_L}\right)^{-1}$$

The obtained values of pressure drops and modified temperatures associated with evaporator and condenser are given below-

**For Benzene:**

$$T_3 = 329.48K$$

$$\Delta P_3 = 813.999Pa$$

$$T_8 = 458.968K$$

$$\Delta P_8 = 51238.237Pa$$

**For Toluene:**

$$T_3 = 357.968K$$

$$\Delta P_3 = 783.170Pa$$

$$T_8 = 460.796K$$

$$\Delta P_8 = 25162.633Pa$$

Assuming all other state points and properties to be same as in the case without pressure drop.

## 5.2 Applying Motinski heat transfer coefficient correlation

Earlier we have used various correlations for heat transfer coefficient as given in the paper. Here, in the second stage of validation, we incorporated one of the nucleate boiling regime correlations. It has been found out in a study that nucleate boiling heat transfer correlation shows better results for heat transfer coefficient of plate heat exchanger. Hence, we used Motinski correlation for the same.

$$h_{nb} = 0.00417 * q^{0.7} * P_{crit}^{0.69} * F_p$$

$$F_p = 1.8p_r^{0.17} + 4p_r^{1.2} + 10p_r^{10}$$

where  $h_{nb}$  is heat transfer coefficient in nucleate boiling regime and unit is  $W/m^2K$ ,  $q$  in  $W/m^2$  and  $P_{crit}$  in kPa.

The obtained values of heat transfer coefficient of evaporator and condenser with both the working fluids Benzene and Toluene are given below.

**For Benzene-**

Evaporation heat transfer coefficient=  $14750.497 W/m^2K$

Condensation heat transfer coefficient=  $7437.722 W/m^2K$

**For Toluene-**

Evaporation heat transfer coefficient=  $10694.308 W/m^2K$

Condensation heat transfer coefficient=  $6405.0336 W/m^2K$

### 5.3 Estimated Component Area

Using the above heat transfer coefficient values we also calculated the heat transfer areas of evaporator and condenser with both the working fluids Benzene and Toluene and obtained the following results:

**For Benzene-**

Area of Evaporator=  $107.030 m^2$

Area of Condenser=  $227.057 m^2$

**For Toluene-**

Area of Evaporator=  $109.649 m^2$

Area of Condenser=  $228.301 m^2$

## 6 Conclusion

This has been observed that the heat transfer coefficient for evaporator and condenser follow a similar trend for Han et al. correlation with both Benzene and Toluene. We have calculated the heat transfer area of the evaporator and condenser using the boiling heat transfer correlation of Kim et al. and the condensation heat transfer correlation of Yan et al. The results of the same obtained by us vary marginally with that in the paper due to various reasons such as fouling factor which we have considered in the order of  $10^{-4}$ , the properties of exhaust gas (such as density, viscosity, specific heat capacity) are considered unchanged at atmospheric pressure. Overall heat



transfer coefficient and the area of each component are found out to be comparable for both Benzene and Toluene. The highest area is occupied by the condenser followed by the evaporator. The heat transfer area occupied by the preheater and the superheater are the least and approximately equal to each other.

When we take the pressure drops into account, we observe a significant change in the heat transfer areas of evaporator and condenser. The component areas of both the evaporator and condenser shrinks by a percentage of 17.4 and 7.3 respectively. This happens because as pressure drop increases, it causes a decrease in the density, mass flow rate and evaporation effect of the working fluid. This accords for the reduction of evaporator capacity and hence their area. This pressure drop is highly dependent on the working fluid velocity. In the condenser, this velocity of the working fluid falls down due to condensation. Therefore the pressure drop effect in the condenser section is considerably lesser than that in the evaporator section. This also reveals that the pressure drop in the evaporator can be minimized by lowering the working fluid velocity between the points 7 and 8.

It is also observed that the component heat transfer areas of evaporator and condenser obtained by the Benzene are slightly less than that obtained in the case of Toluene. This slight difference may arise due to the usage of different heat transfer correlations for predicting the heat transfer area.

We can conclude with the fact that here, the areas obtained using the plate heat exchanger is lower and higher heat transfer coefficient is achieved as in contrast to the other type of heat exchangers such as the Shell and Tube heat exchanger. Hence, the plate heat exchanger is the most effective in extracting the waste heat energy.

## References

- [1] Organic rankine cycle [online],. <http://www.ormat.com/organic-rankine-cycle>, ormat,2015.
- [2] Hannu Jaaskelainen. Diesel exhaust gas. [www.dieselnet.com](http://www.dieselnet.com).
- [3] Tae-Woo Lim, Yong-Seok Choi, and Chun-Ki Lee. Design of plate heat exchangers for use in medium temperature organic rankine cycles. *Heat and Mass Transfer*, 55(1):165–174, 2019.

## **7 Annexure**